

**Dephasing of intersublevel polarizations in InAs/GaAs self-assembled quantum dots**

S. Sauvage, P. Boucaud,\* and T. Brunhes

*Institut d'Electronique Fondamentale, Bâtiment 220, Université Paris-Sud, 91405 Orsay, France*

M. Broquier and C. Crépin

*Laboratoire de Photophysique Moléculaire, Bâtiment 210, Université Paris-Sud, 91405 Orsay, France*

J.-M. Ortega

*CLIO/LURE, Bâtiment 209 D, Université Paris-Sud 91405 Orsay, France*

J.-M. Gérard

*CEA-Grenoble, DRFMC-PSC, 38054 Grenoble Cedex 9, France*

(Received 19 December 2001; revised manuscript received 25 July 2002; published 23 October 2002)

We have performed time-integrated degenerate four-wave mixing experiments in InAs/GaAs self-assembled quantum dots. The quantum dots are excited in resonance with an intersublevel transition between the valence states of the dots. The dephasing time  $T_2$  is deduced from the time dependence of the photon echo amplitude as a function of the delay between the two incident pulses. At low temperature, a dephasing time  $T_2$  of 15 ps is measured for a resonant excitation at  $7.4 \mu\text{m}$  wavelength. This dephasing corresponds to an homogeneous broadening of the intersublevel transition of  $87 \mu\text{eV}$ . The polarization decay time is much longer than the one observed for resonant intersubband excitations in quantum wells. The dephasing time of the intersublevel polarization exhibits only a weak temperature dependence, indicating that the dephasing is not dominated by phonon-assisted scattering mechanisms.

DOI: 10.1103/PhysRevB.66.153312

PACS number(s): 78.67.Hc, 78.47.+p, 42.50.Md

The coherent interaction between semiconductor quantum dots and optical excitations is a key feature for coherent control<sup>1</sup> and quantum information processing with nanostructures.<sup>2</sup> The dynamic of carriers and the carrier relaxation in the dots have been extensively studied, both theoretically<sup>3–5</sup> and experimentally.<sup>6–8</sup> The phase relaxation processes are a challenging issue less straightforward to tackle: an ensemble of semiconductor self-assembled quantum dots is characterized by a strong inhomogeneous broadening due to the dot size and shape distribution. This inhomogeneous broadening prevents the measurement of the dephasing time from the spectral linear response of the ensemble. For interband excitations, the dephasing times can be measured by local spectroscopy techniques.<sup>9</sup> Near-field optical microscopy techniques can provide the homogeneous broadening of localized excitons.<sup>10</sup> These experimental data give information on the dephasing mechanisms, including carrier-carrier interaction, phonon interaction, or lifetime broadening. The measurement of the excitonic dephasing in semiconductor quantum dots and of the exciton optical linewidth in individual quantum dots can be compared to the theoretical predictions to identify the phase breaking processes.<sup>11,12</sup> In the case of InAs/GaAs self-assembled quantum dots, the dephasing associated with an interband excitation was measured by spectral-hole burning, transient four-wave mixing (FWM) and wave-packet interferometry techniques.<sup>13–16</sup> Dephasing times ranging between 300 fs at room temperature and 630 ps at low temperature were reported. FWM experiments were also performed to measure the phase relaxation time in CdSe nanocrystals.<sup>17</sup>

Doped semiconductor heterostructures can also be excited resonantly in the midinfrared spectral range. In this case, the

excitation corresponds to an unipolar mechanism with either electrons or holes. The intraband excitations are either resonant with intersubband transitions in quantum wells or with intersublevel transitions in quantum dots.<sup>18</sup> In semiconductor quantum wells, the decay of intersubband coherent polarizations was analyzed by femtosecond FWM in the midinfrared.<sup>19,20</sup> Electron-electron scattering in the two-dimensional electron plasma was cited as the main source of dephasing. To our knowledge, the dephasing times associated with an intersublevel excitation in self-assembled quantum dots has not been investigated.

In this work, we report degenerate FWM experiments in resonance with midinfrared intersublevel transitions to study phase relaxation in self-assembled quantum dots. An intersublevel transition around  $7.4 \mu\text{m}$  wavelength between the valence states of the quantum dots is excited resonantly in the midinfrared with a picosecond free-electron laser. The photon echo is measured as a function of the time delay between the incident pulses and the dephasing time is deduced from the time decay of the coherent polarization. At low temperature, the intersublevel dephasing time is found equal to 15 ps. This dephasing time in quantum dots is considerably longer than the one reported for intersubband excitations in quantum wells. The polarization decay time is only weakly temperature dependent up to room temperature, thus ruling out phonon-assisted mechanisms as the origin of the dephasing. These features illustrate the specific phase relaxation properties associated with the three-dimensional confinement in semiconductor quantum dots.

The InAs/GaAs self-assembled quantum dots were grown by molecular-beam epitaxy. The investigated sample was previously used for different harmonic generation experi-

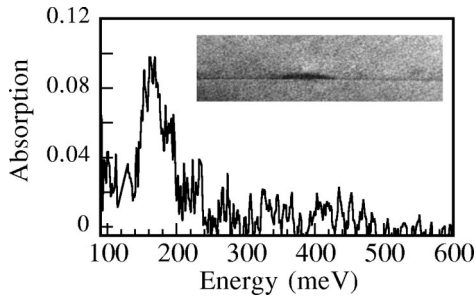


FIG. 1. Midinfrared absorption in TE polarization of the waveguide containing  $p$ -doped self-assembled quantum dots. The transmission of the waveguide is normalized by the transmission of a waveguide with undoped quantum dots. The experiment is performed at room temperature. The inset shows a cross-section transmission-electron microscopy image of an InAs/GaAs self-assembled quantum dot. The dot size corresponds to a height of 2.5 nm and a base diameter of 25 nm.

ments in resonance with intersublevel transitions.<sup>21,22</sup> The quantum dots are modulation doped with a  $\delta$  doping with a nominal concentration of  $6 \times 10^{10} \text{ cm}^{-2}$  lying 2 nm above the wetting layer. Only the ground state of the quantum dots is populated. The areal dot density is estimated to be around  $4 \times 10^{10} \text{ cm}^{-2}$ . The vertical stacking of the quantum dot layers consists of 40 InAs quantum dot layers separated by 35-nm-thick GaAs barriers. To increase the interaction length with the midinfrared light, the quantum dot layers are embedded in a waveguide. The optical confinement is provided by a midinfrared waveguide, grown on a heavily doped ( $2 \times 10^{18} \text{ cm}^{-3}$ ) GaAs substrate, which consists of a  $\text{Al}_{0.9}\text{Ga}_{0.1}\text{As}$  5  $\mu\text{m}$ -thick cladding layer followed by a 1.8  $\mu\text{m}$  thick GaAs layer, the active region with the quantum dot layers, and a 2.3  $\mu\text{m}$  GaAs top layer.<sup>23</sup> The photon echo measurements were performed with a free-electron laser as the optical excitation. The free-electron laser delivers macropulses with a duration of 10  $\mu\text{s}$  at a repetition rate of 25 Hz. Each macropulse is constituted of micropulses with a variable duration that can be adjusted down to 0.5 ps at a repetition rate of 32 MHz. The copolarized infrared beams with wave vectors  $\mathbf{k}_1$  and  $\mathbf{k}_2$  are focused with a 15-cm parabolic mirror (spot size  $\sim 300 \mu\text{m}$  diameter) and injected in a non-collinear geometry through the cleaved facet of the waveguide with different incidence angles. The energy of the probe pulse incident on the sample with wave vector  $\mathbf{k}_2$  is around 2.5  $\mu\text{J}$ . In an inhomogeneously broadened system, for a delay time  $\tau$  between the two incident pulses, a photon echo is emitted after the phase restoration in the direction  $2\mathbf{k}_2 - \mathbf{k}_1$  at a time delay of  $2\tau$ . The amplitude of the photon echo was measured as a function of the delay between the incident pulses with a mercury-cadmium-telluride photodetector. Bulk GaAs or Si samples excited at normal incidence were used as reference samples for the echo experiment.

Figure 1 shows the midinfrared absorption spectrum of the  $p$ -doped quantum dot sample measured at room temperature in TE polarization (polarization in the layer plane of the dots). The absorption was measured with a microscope coupled to a Fourier-transform infrared spectrometer. The transmission of the waveguide quantum dot sample was nor-

malized by the transmission of a similar waveguide sample with undoped quantum dots. In TE polarization, the absorption is resonant around 165 meV with a full width at half maximum of 30 meV. The amplitude of the absorption after a 3 mm propagation length is 7.5%. An experimental dipole matrix element of 0.14 nm is deduced for this intersublevel transition. In TM polarization (polarization along the growth axis of the quantum dots), the absorption is dominated by a strong resonance around 100 meV with a 36 meV broadening.<sup>21</sup> Separate measurements have shown that the amplitude of the absorption increases by a factor of 2 when the temperature of the sample is decreased down to 10 K. This feature indicates a more efficient charge transfer into the dots at low temperature.

The confined valence energy states in the quantum dots were calculated by solving the three-dimensional Schrödinger equation in the effective-mass approximation.<sup>22</sup> This calculation accounts for the flat lens shape of the quantum dots, as shown in the inset of Fig. 1. To comply with the experiment, an InAs quantum dot with a 4.5 nm height and a 25 nm base diameter embedded in a GaAs matrix was considered. A  $z$ -polarized intersublevel transition resonant around 110 meV between the ground state  $h_1$  and the seventh confined state  $h_7$  is deduced with this geometry.<sup>24</sup> This transition has a 0.36 nm dipole matrix element and corresponds to the dominant absorption observed in TM polarization. At higher energies, two in-plane polarized transitions between  $h_1$  and  $h_{8,9}$  and between  $h_1$  and  $h_{13,14}$  are predicted at 133 and 188 meV, respectively. The  $h_1$ - $h_{8,9}$  intersublevel transition has an in-plane dipole matrix element of 0.13 nm while the  $h_1$ - $h_{13,14}$  intersublevel transition has a 0.25 nm dipole matrix element. The uncertainty on the quantum dot structural parameters (size, composition) and a single-band three-dimensional effective-mass calculation do not allow an unambiguous assignment of the intersublevel transition at 165 meV. We note that the calculation predicts intersublevel transitions with strong in-plane dipole matrix elements as observed experimentally in an energy window of 30 meV around the experimental resonance. Additional information on the electronic structure of the dots was obtained by second-harmonic generation experiments, which have shown a resonant enhancement of the second-harmonic power around 168 meV with a 4 meV broadening for a TE polarized excitation. This enhancement of the second-order nonlinear susceptibility  $\chi_{xxx}^{(2)}$  was associated with the achievement of the double resonance between the infrared excitation and the intersublevel transitions.<sup>22</sup> We emphasize that the energy differences between  $h_{8,9}$  or  $h_{13,14}$  and the closest confined states are around 14 and 6 meV, respectively. The calculation indicates that the confined states are relatively well separated, i.e., there is the absence of a continuum of states close to the confined states involved in the echo experiments.

Figure 2 shows the FWM signal for a reference GaAs sample and for the  $p$ -doped quantum dot sample. The measurement was performed at low temperature (5 K). The in-plane polarized excitation was set at 168 meV. In the case of the bulk GaAs sample excited far from a resonance, the dephasing occurs on a very short-time scale ( $T_2 \sim 1/\omega$ , where  $\omega$  is the excitation pulsation).<sup>25</sup> The duration of the

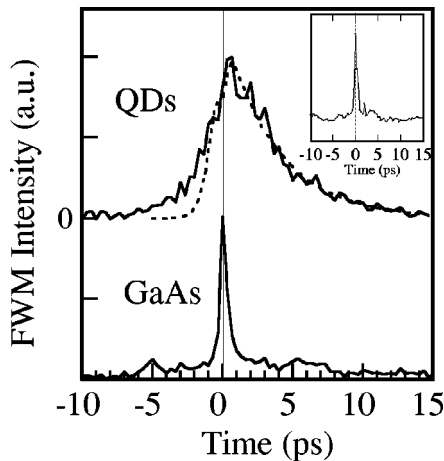


FIG. 2. Low-temperature (5 K) time-integrated FWM signal obtained at  $7.4 \mu\text{m}$  (168 meV) with a GaAs reference sample (lower curve) and the quantum dot sample (upper curve). The lower curve has been offset for clarity. The dashed line corresponds to the theoretical FWM signal associated with a dephasing time of 15 ps. The delay corresponds to the delay between the two exciting pulses. The measurement is performed at low temperature (5 K). The inset depicts the FWM signal for an excitation wavelength of  $7.0 \mu\text{m}$  in the quantum dot sample.

FWM signal is therefore limited by the temporal pulse width. A Gaussian excitation pulse width of 0.5 ps is deduced from this FWM signal according to the calculation explained in the following. In the case of the quantum dot sample a FWM signal considerably longer than the pulse width is measured. In addition, there is a significant signal at negative delay that is not compatible with the finite 0.5 ps pulse duration. In homogeneously broadened systems, the polarization at a pulsation  $2\omega$  can induce an echo at negative time delays with a characteristic time decay of  $T_2/2$ .<sup>26</sup> The decay becomes shorter at negative time delays as the inhomogeneous broadening increases.<sup>27</sup> The observation of a long FWM signal along with a negative-delay component was only observed for a resonance excitation around  $7.4 \mu\text{m}$  wavelength (168 meV), which corresponds to the strongest resonance associated with second-harmonic generation.<sup>22</sup> The same experiment performed out of this resonance at 7- and at 11–12- $\mu\text{m}$  wavelength only showed a symmetric FWM signal limited by the pulse duration. The inset of Fig. 2 shows the FWM signal measured for a  $7 \mu\text{m}$  excitation. At  $7 \mu\text{m}$ , the contribution of GaAs is dominant as compared to the one of the quantum dots. The difference between 7.4 and  $7 \mu\text{m}$  indicates that the measured echo is not associated with a chirped propagation through the GaAs waveguide. This point is further reinforced by the satisfying agreement between the experiment and the theory as explained below.

In order to, first, extract to dephasing time  $T_2$  with a pulse of finite duration and, secondly, account for the negative-delay signal in Fig. 2, the time-integrated FWM signal was calculated within the formalism reported in Ref. 27. At positive time the photon echo is essentially the result of the third-order interaction of the pump and probe pulses. At negative delay, where the previous contribution is vanishing because of the short pulse duration, the echo results from the interac-

tion of the electric field of the pump beam with the coherent second-order polarization at  $2\omega$  created by the probe beam. We have considered Gaussian pulse excitations and numerically calculated the total third-order polarization that radiates the echo. Because of the multiple integrals, special care was devoted to ascertain the validity of the successive numerical integrations. The inhomogeneous broadening involved for the single resonant polarizations is 30 meV. However, the relevant broadening associated with the resonant enhancement of the second harmonic is not the broadening of the absorption but rather the spectral width of the double resonance, which is much smaller. In the calculation, we considered for the latter one a 0.5 meV broadening, in reasonable agreement with the theoretical 1 meV value reported in Ref. 22 (note that the experimental data at room temperature in Ref. 22 are limited by the sampling). This broadening has to be compared with the upper value of 0.6 meV reported for resonant second-harmonic generation between the conduction states of  $n$ -doped quantum dots.<sup>28</sup> For the calculation,  $T_1 = T_2/2$  and  $C = 0.038$  were assumed according to notations of Ref. 27. The simulation of the echo intensity is shown in Fig. 2 as a function of the time delay. At positive time, for an inhomogeneously broadened system such as an intersublevel transition in self-assembled quantum dots, the echo decays as  $\exp(-4\pi/T_2)$ . Note that the polarization originating from the double resonance *does not* contribute to the signal at positive delays. A dephasing time  $T_2 \sim 15$  ps is deduced from the decay. At negative delays a satisfying agreement is also obtained from this value.

The value of the dephasing time should first be compared with that reported for intersubband excitations in quantum wells. Typical dephasing times of the order of 200–300 fs were reported by time-integrated FWM experiments<sup>19</sup> performed with a resonant intersubband excitation at 260 meV in  $n$ -doped InGaAs/AlInAs quantum wells. Electron-electron interactions were shown to be the dominant source of dephasing. The dephasing time measured for an intersublevel excitation is almost two orders of magnitude longer. It is attributed to the three-dimensional confinement of the quantum dots. The value of the intersublevel dephasing time is also different from those reported for interband excitations of the quantum dots. Room-temperature measurements in InGaAs quantum dots did show interband dephasing times around 200 fs.<sup>13</sup> The coherent dynamics following an interband excitation of the excited levels was also studied by near-field coherent excitation spectroscopy and wave-packet interferometry.<sup>14,15</sup> In the latter work, various values of  $T_2$ 's up to 90 ps were reported depending on the energy separation between confined levels. These large values of  $T_2$  indicate that phonon emission processes can be significantly quenched due to a strong reduction of available phase space. A dominant dephasing mechanism based on interlevel carrier relaxation was proposed. Since the energy-level separation in these quantum dots was of the order of a few meV, the intersublevel carrier relaxation was found to be assisted by longitudinal-acoustical phonons.

The dephasing time measured in the present experiment corresponds to an homogeneous broadening at full width at half maximum of the intersublevel transition  $\Gamma = 2\hbar/T_2$



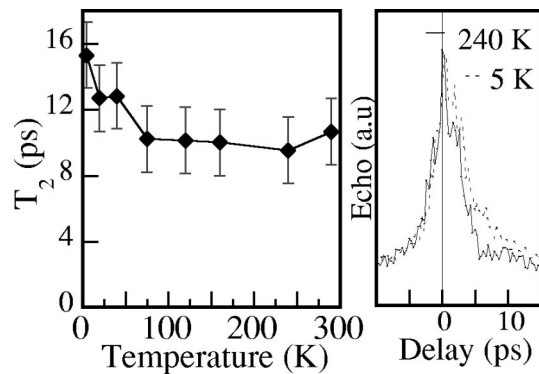


FIG. 3. Dephasing time associated with an intersublevel excitation at  $7.4 \mu\text{m}$  as a function of the lattice temperature (left). The full curve is a guide to the eyes. The right curve shows a comparison of the echo signal at 5 and 240 K.

$\sim 87 \mu\text{eV}$ . We emphasize that this FWM experiment provides measurement of the homogeneous broadening of an intersublevel transition in InAs/GaAs self-assembled quantum dots. The average  $87 \mu\text{eV}$  linewidth has to be compared, for example, with the 4 meV linewidth measured by time-integrated FWM experiments in resonance with intersubband excitations around 100 meV in high-quality GaAs/AlGaAs quantum wells.<sup>20</sup>

Figure 3 shows the temperature dependence of the dephasing time measured for an excitation at 168 meV. The striking feature is that the dephasing time only exhibits a weak temperature dependence up to room temperature. This temperature dependence is in sharp contrast with the one usually observed for interband excitations or that is theoretically predicted.<sup>12</sup> In the case of interband excitations in InGaAs self-assembled quantum dots, long dephasing times have been measured at low temperature.<sup>13</sup> Meanwhile a stronger temperature dependence was observed, with dephasing times decreasing from 630 ps at low temperature to 200

fs at room temperature. The dephasing associated with an intersublevel excitation is more robust versus the temperature. This lower sensitivity implies that the dephasing time is longer at room temperature as compared to the dephasing time of interband excitations, even if it is shorter at low temperature.

The question arises as to whether the dephasing is associated with population relaxation or pure dephasing process. The lack of a strong temperature dependence as shown in Fig. 3 rules out the role of phonons as the main source of dephasing in the single-particle electronic picture. Alternate dephasing mechanisms associated with carrier interactions or impurity scattering could be at the origin of the decay of the intersublevel polarization. The measurement of the dephasing times indicates a slowing of the intersublevel energy relaxation as compared to two-dimensional systems since the phase relaxation occurs either by population relaxation ( $1/2T_1$ ) or by a pure dephasing rate. The present FWM measurements indicate that the intersublevel relaxation time is longer than 7.5 ps ( $T_1 = T_2/2$ ). We note that this lower limit of the relaxation time remains one order-of-magnitude shorter than the energy relaxation time measured between the ground conduction state and the first excited conduction state in InAs/GaAs quantum dots.<sup>29</sup>

In conclusion, we have investigated the dephasing of intersublevel polarizations in InAs/GaAs self-assembled quantum dots. Time-integrated FWM experiments in resonance with valence intersublevel transitions were performed. A dephasing time of 15 ps was measured for a resonant unipolar excitation between valence states at 168 meV. This dephasing time is significantly longer than the dephasing times reported for intersubband polarization in quantum wells. It corresponds to an homogeneous broadening of the intersublevel transition of  $87 \mu\text{eV}$ . The dephasing time shows only a weak temperature dependence. This feature indicates that the dephasing of the intersublevel polarizations in the quantum dots is not assisted by a phonon-mediated process.

\*Electronic mail: philippe.boucaud@ief.u-psud.fr

<sup>1</sup>N. H. Bonadeo *et al.*, *Science* **282**, 1473 (1998).

<sup>2</sup>A. Barenco, D. Deutsch, A. Ekert, and R. Josza, *Phys. Rev. Lett.* **74**, 4083 (1995).

<sup>3</sup>U. Bockelmann and T. Egeler, *Phys. Rev. B* **46**, 15 574 (1992).

<sup>4</sup>H. Benisty, C. M. Sottomayor-Torrès, and C. Weisbuch, *Phys. Rev. B* **44**, 10 945 (1991).

<sup>5</sup>X-Q. Li and Y. Arakawa, *Phys. Rev. B* **56**, 10 423 (1997).

<sup>6</sup>Y. Toda, O. Moriwaki, M. Nishioka, and Y. Arakawa, *Phys. Rev. Lett.* **82**, 4114 (1999).

<sup>7</sup>S. Sauvage *et al.*, *Appl. Phys. Lett.* **73**, 3818 (1998).

<sup>8</sup>J. Urayama, T. B. Norris, J. Singh, and P. Bhattacharya, *Phys. Rev. Lett.* **86**, 4930 (2001).

<sup>9</sup>J. Y. Marzin *et al.*, *Phys. Rev. Lett.* **73**, 716 (1994).

<sup>10</sup>D. Gammon *et al.*, *Science* **273**, 87 (1996).

<sup>11</sup>T. Takagahara, *Phys. Rev. B* **60**, 2638 (1999).

<sup>12</sup>X-Q. Li and Y. Arakawa, *Phys. Rev. B* **60**, 1915 (1999).

<sup>13</sup>P. Borri *et al.*, *Phys. Rev. B* **60**, 7784 (1999).

<sup>14</sup>H. Htoon *et al.*, *Phys. Rev. B* **63**, 241303 (2001).

<sup>15</sup>Y. Toda, T. Sugimoto, M. Nishioka, and Y. Arakawa, *Appl. Phys. Lett.* **76**, 3887 (2000).

<sup>16</sup>P. Borri *et al.*, *Phys. Rev. Lett.* **87**, 157401 (2001).

<sup>17</sup>R. W. Schoenlein *et al.*, *Phys. Rev. Lett.* **70**, 1014 (1993).

<sup>18</sup>H. Drexler *et al.*, *Phys. Rev. Lett.* **73**, 2252 (1994).

<sup>19</sup>R. A. Kaindl *et al.*, *Phys. Rev. Lett.* **80**, 3575 (1998).

<sup>20</sup>R. A. Kaindl *et al.*, *Phys. Rev. B* **63**, 161308 (2001).

<sup>21</sup>S. Sauvage *et al.*, *Phys. Rev. B* **59**, 9830 (1999).

<sup>22</sup>T. Brunhes *et al.*, *Phys. Rev. B* **61**, 5562 (2000).

<sup>23</sup>J. P. Galaup *et al.*, *J. Lumin.* **86**, 363 (2000).

<sup>24</sup>The spin degeneracy is not taken into account in the indexing of the confined states.

<sup>25</sup>P. N. Butcher and D. Cotter, *The Elements of Nonlinear Optics* (Cambridge University Press, Cambridge, England, 1990).

<sup>26</sup>J. P. R. Wells *et al.*, *Phys. Rev. Lett.* **84**, 4998 (2000).

<sup>27</sup>B. F. Feuerbacher, J. Kuhl, R. Eccleston, and K. Ploog, *Solid State Commun.* **74**, 1279 (1990).

<sup>28</sup>S. Sauvage *et al.*, *Phys. Rev. B* **63**, 113312 (2001).

<sup>29</sup>S. Sauvage *et al.*, *Phys. Rev. Lett.* **88**, 177402 (2002).